Spatial-temporal Analysis of Landslides in Complex Hillslopes of Catchments Using Dynamic Topmodel

F.Bahmani1 , M.H.Fattahi[1] , T.Sabzevari[2]* , A.Torabi Haghighi[4] , A.Talebi[3]

[1] Department of civil engineering, Marvdasht Branch, Islamic Azad University, Marvdasht, Iran

[2] Department of civil engineering, Estahban Branch, Islamic Azad University, Estahban, Iran

[3] Faculty of Natural Resources, Yazd University, Yazd, Iran

[4] Water, Energy and Environmental Engineering Research Unit, University of Oulu, Finland

* Corresponding Author: tooraj.sabzevari@gmail.com

Abstract

Hillslopes of the catchments in nature have three forms (convergent, divergent, parallel) in terms of plan shape and also in terms of floor curvature profile, they have three convex, concave, and straight shapes combining into complex hillslopes. Previous studies indicated the topography and geometry of complex hillslopes influence their hydrologic responses/attributes in both surface and subsurface flow. The three-dimensional shape and geometry of the hillslopes were introduced into Topmodel as the new parameters, and a complex Topmodel was presented that could check the saturation of different parts of complex hillslopes. The complex Topmodel model was linked to the landslide model “SINMAP”. Finally, the spatial-temporal variations of the saturation of the complex hillslopes and their stability rate were investigated using the Dynamic Topmodel. Results revealed that the influence of local slope, which is a function of curvature of the hillslopes, is more dominant than the saturation rate on the stability of the hillslopes. In contrast with convex hillslopes, the downstream in the concave hillslopes were more stable than upstream. Nevertheless, the upstream area in the concave hillslopes and downstream in the convex ones can be prioritized to implement artificial stabilization.

Keywords: Topography, complex hillslope, landslide, SINMAP, Dynamic Topmodel

1. Introduction

Landslide is a natural or artificial instability in slopes that can occur due to local geological, hydrological, or geomorphological conditions. It can be triggered by human activities such as land use and topography changes and might be intensified by natural phenomena such as extreme rainfall and earthquakes.

Landslide is a geodynamic process usually takes place in the top layers of the earth and is considered a serious threat to life and property in many parts of the globe. Understanding the different types of landslides and the process of their formation, influential factors in creating mass movements and recognizing the most landslide-prone areas, and estimating their risk is among the most critical initiatives to minimize the effects of this type of natural hazard. Various factors such as topography, climate, and weathering with different levels of contribution play a role in the occurrence of these movements. Identifying these factors, which significantly helps in attributing risk to different areas, is among the most necessary measures to prevent and reduce damage. Hence, the strategy of landslide study includes having a sound understanding of involving processes, risk analysis, and derivation of landslide susceptibility maps.

Figure 1: A landslide in a road located in a suburban area

Annually, many natural hillslopes are devastated by landslides and usually lead to considerable economic and non-economic losses, particularly nearby infrastructures, villages, and cities (Dilley et al., 2005; Kjekstad and Highland, 2009; Lin and Wang, 2018). Landslides account for 5.5% of natural hazards (2009-2018), contributing to 1.6% of the death tolland 0.11% of the economic damage among natural hazards (CRED, 2020). Increasing the frequency of severe storms induced by climate change and human activities (e.g., road construction, deforestation and urbanization) in high-risk areas are reckoned as the main culprits in the landslide tragedies of the world (Dai et al., 2002). Figure 1 shows an example of landslides on roads in residential areas.

Several stability models such as CHASM, SHALSTAB, SINMAP, TRIGRS, SHETRAN, GEOTOP-FS and SUSHI are widely used to scrutinize the stability of catchment hillslopes. Out of these, the Shalstab Stability Model (SHALSTAB) (Dietrich, Montgomery 1998) and the Stability Index Model (SINMAP) (Pack et al., 1998) have analogous structures with considering hydrological, geomorphological, and geotechnical features.

SINMAP (Stability Index Mapping) model proved to be highly reliable in predicting slope instabilities as introduced by Tarboton and Pack (1997), and Tarboton and Goodwin (1999). It works based on the infinite slope stability model and has been widely used under various geological and hydrological conditions (Tarolli and Tarboton, 2006; Preti, 2015; Letterio and Rabonza et al., 2016).

The compatibility and accuracy of the SINMAP model were tested by Zizioli et al. (2013) by comparing its performance with other models such as SHALSTAB, TRIGRS, and SLIP. They concluded that all models have almost the same accuracy, considering that the SINMAP is developed based on the saturation rate of the hillslopes. It is worth mentioning that during rainfall, changes in the degree of soil saturation and increase in pore water pressure lead to decreasing shear soil strength and sliding the slopes.

Variation of saturation degree in hillslopes depends on soil characteristics, rainfall recharge rate, hillslopes' topography, and soil moisture content (O'loughlin, 1986; Ogden and Watts, 2000; Sabzevari et al., 2010; Ardekani and Sabzevari, 2020). The hydrological models consider the role of precipitation and infiltration to simulate subsurface flow and saturation of the hillslopes, and the landslide models describe the stability of the hillslopes based on data from the hydrological models (Montgomery and Dietrich, 1994; Wu and Sidle, 1995; Borga et al., 2002; Arnone et al., 2011). TOPMODEL is a subsurface hydrological model that helps to determine the degree of soil moisture deficit (SMD) until the saturation phase for different parts of the hillslopes. The runoff mechanism governing this model is the Dunne-Black mechanism in which the subsurface flow beneath the soil surface saturates the soil and controls the moisture content at each pixel of the hillslope. TOPMODEL can characterize the spatial distribution of moisture and SMD over the whole catchment area and locate the catchment points where saturation is likely to occur. In Dunne-Black mechanism, surface flow originates from the saturation points of the hillslopes (Dunne and Black, 1970). TOPMODEL uses a topography index $[\lambda = \ln(\frac{a}{S})]$ (a and S are specific catchment area and local slope) computable for each hillslope point. It implicitly compares the subsurface water accumulating at a given point of hillslope and subsurface water passing through the same point based on the hillslopes' topography. As the saturation degree increases in a part of the hillslopes, the pore water pressure increases too and the resistant shear stress of the soil attenuates, and it is the weight force that brings about rupture and landslide at that point on the hillslope (Bishop, 1959; Campos et al., 1994; Godt et al., 2009).

The topography of hillslope plays a significant role in its saturation rate. Natural hillslopes have different geometry. They can be categorized as convergent, parallel, or divergent in plan shape and have concave, flat, or convex shapes in terms of the degree of curvature of their profile. by combining the plan shapes and profile curvatures, nine distinct geometries can be considered for the hillslopes called “complex hillslopes”. Ragers and Sitar, (1993) stated that natural hillslopes have different curvatures, and landslides occur mainly on sloping or concave hillslopes. Park et al. (2001) considered the effect of topography by classifying complex hillslopes into six groups. Extensive research has been conducted about the effect of hillslope geometry on subsurface flow and the degree of saturation of complex hillslopes (Ogden and Watts, 2000; Troch et al., 2002, 2003; Aryal et al., 2005 ; Berne et al., 2005 ;Talebi et al., 2008 ; Sabzevari et al., 2010 ; Sabzevari and Noroozpour, 2014 ; Liang and Chan, 2017 ; Fariborzi et al., 2019 ; Pishvaei et al., 2020). Sabzevari et al. (2010) suggested equations for estimating the saturation zone length and saturation rate of 9 complex hillslopes. According to their results, convergent and concave hillslopes tended to be more saturated than divergent and convex ones. Talebi et al. (2008) presented a steady-state analytical slope stability model to investigate the role of topography in rain-induced shallow landslides. They combined a continuous two-variable performance of the topographic surface, a steady-state hydrological model of the hillslope saturation storage to investigate the interaction between geometric features of the earth, saturated storage in the hillslopes, and soil mechanics under the assumption of infinite slope stability. Their results verified that the stability of the hillslopes varies from concave to convex hillslopes and from convergent to divergent hillslopes. Lida (1999) showed that slope angle, topography, and soil depth are important factors that control landslides. During the study of the effect of geological factors on shallow landslides in the Apuna mountainous region in northwestern Tuscany, Italy, Avanzi et al. (2004) stated that bedrock and impermeability were key issues in the occurrence of landslides. Accordingly, it was stated that 56% of the reported landslides occurred in hollow (concave) surfaces, 38% in flat surfaces and the remaining 6% on convex surfaces.

Pishvaei et al. (2020) developed the TOPMODEL equations and considered the role of complex hillslopes’ topography in their saturation. In their study, the complex hillslope model was combined with the SCS-CN model, and the effects of hillslope geometry upon infiltration rate and parameters of infiltration such as curve number were investigated. They concluded that the convergent slops had 15.4% less infiltration and divergent hillslopes had 7.8% more infiltration than parallel ones. The infiltration rate on concave hillslopes was 13.5% less and the infiltration rate on convex hillslopes was 5.8% more than the straight cases. The degree of convergence/divergence had more effects on CN than profile curvature. Sabzevari and Talebi (2021) introduced the relationship between the SINMAP and TOPMODEL and explored their parameters. In this regard, the data of the catchment area of Ilam Dam, southeast of Ilam province, Iran, was used. The variation of SMD and saturation index were mapped with the help of GIS and based on TOPMODEL before the SINMAP stability maps for the region were calculated. Most reported studies to show that convergence in the topography of the area and the slope angle play the most imperative role in the commencement of shallow landslides (Montgomery and Dietrich, 1994; Fernandes et al., 2004; Talebi et al., 2008).

Talebi et al. (2008) mixed the hillslope-storage Boussinesq model (HSB) with the infinite slope stability method. Solutions of the HSB equation indirectly take into account plan shape by introducing the hillslope width function and profile curvature through the bedrock slope angle and the hillslope soil depth function. The suggested model is constituted of three sub-models: (1) a topography model hypothesizing three-dimensional soil mantled landscapes, (2) a dynamic hydrology model for shallow subsurface flow and water table depth (HSB model), and (3) an infinite slope stability technique based on the Mohr-Coulomb failure law. Results indicated that after a limited period of rainfall, the convergent hillslopes with concave and straight profiles

become unstable faster than others, whereas the divergent convex hillslopes keep their stability (even after rainfall intensity is increased).
Dynamic TOPMODEL, developed later by Beven and Freer (2001), uses kinematic wave routing for subsurface flows between classes of points similar in hydrological terms, where the classification is based on $a/\tan\beta$ index. Since then, Dynamic TOPMODEL has been used in several studies such as the catchments of Panola (Peters et al., 2003), Plynlimon (Page et al., 2007), Maimai (Beven and Freer, 2001; Freer et al., 2004), Attert (Liu et al., 2009), and Brompton (Metcalfe et al., 2017).
In the current research, in the first place, the governing equations of TOPMODEL have been developed and reformulated so that it can directly consider the combined effects of plan shape and surface curvature of complex hillslopes. Then based on the resulting model, named Complex TOPMODEL, the SMD values along the slopes were estimated, and, finally, this model was combined with the SINMAP stability model to investigate, among other things, the stability values of different points of the complex hillslopes concerning time. To evaluate the stability of hillslopes in the unstable mode, a Dynamic topmodel was utilized.

Figur2: A scheme of a convergent hillslope (Mirkazemian, 2018)

2. SINMAP Landslide Model

Figure 2 depicts a convergent hillslope located at Tar Lake, Damavand city, Tehran, Iran, which experienced a rainfall-induced landslide due to inadequate plant coverage.
Nowadays, various statistical, descriptive, and process-based methods predict landslides. Most studies in Iran are based on statistical and descriptive methods. The statistical zonation models are mainly based on the density of landslides per unit area. The accuracy of such models can be enhanced by increasing the computational layers involved in the model. However, deterministic models such as SINMAP are based on numerical calculations and relatively precise physical parameters. SINMAP was suggested by Tarboton and Pack (1997) and Tarboton and Goodwin (1999) based on the infinite slope stability model. The SINMAP model has been tested by several researchers under different geological and hydrological conditions (Tarolli and Tarboton, 2006; Preti and Letterio, 2015; Rabonza et al., 2016) and was proved to lead to reliable results in predicting slope instabilities. One of the salient features of the SINMAP software model is that computations are based on a grid-cell network. This model integrates a hydrological model and a physical model of slope stability, the results of which could be practically more helpful in calculating the stability index compared to other similar models.
Figure 3 shows a sloping surface where the subsurface flow occurs through the hillslope. The soil depth and the subsurface flow depth are denoted as D and Dw, respectively. Also, the values of soil depth and flow in the direction perpendicular to the impervious surface area, respectively, hw and h.

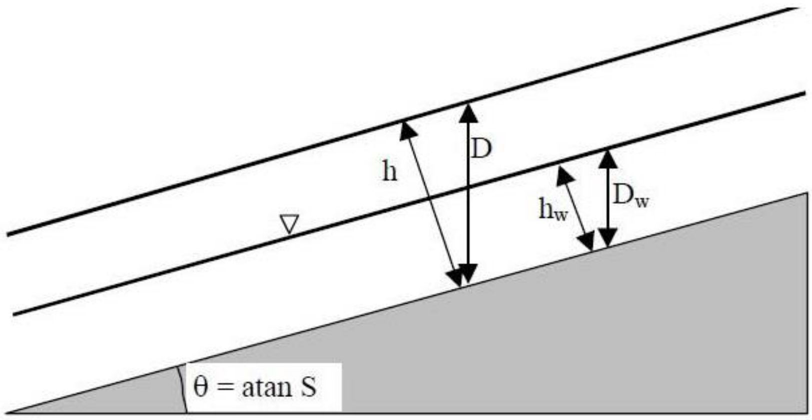

Figure 3: A sloping surface with the subsurface flow (Goodwin and Pack, 2012)

In the SINMAP model, the slope stability safety factor is the ratio of the stabilizing force (friction force and soil cohesion) to the destabilizing force (gravity), which is defined as (Pack et al., 1998)

$$FS = \frac{C_r + C_s + cos^2\theta[\rho_s g(D - D_W) + (\rho_s g - \rho_w g)D_W]tan\varphi}{D\rho_s g\ sin\theta cos\theta} \tag{1}$$

where C_r is the root-induced cohesion coefficient [N/m^2], C_s is the soil cohesion [N/m2], θ represents the slope angle, ρ_s is the wet soil density [kg / m^3], ρ_w stands for water mass density [kg/m3], D is the soil depth, and φ designates the internal friction angle. We have also h = Dcosθ and $h_w = D_w \cos\theta$. If the value of δ = Dw / D = hw /h is considered, Eq. (1) is simplified as follows (1998 Pack et al.):

$$Fs = \frac{C + \cos\theta[1 - \delta.r]\tan\varphi}{\sin\theta} \quad : \tag{2}$$

where $r = \frac{\rho_w}{\rho_s}$, $C = \frac{C_r + C_s}{h\rho_s g}$. and δ, is called saturation index (or relative wetness):

$$\delta = \min\left(\frac{R\ a}{T\ \sin\theta}, 1\right) \tag{3}$$

where R is the recharge rate to the subsurface layer, θ is the slope angle, T = K_0 D, (K_0 is the saturated hydraulic conductivity of the soil) and a = A/w is the so-called specific catchment area with w being the flow width at any point on the hillslope and A the upstream drainage area upstream at any point. The maximum value for δ is one; therefore, if δ exceeds 1, its value will be changed to 1. In this situation, we have D = D_w . In other words, the depth of the subsurface flow is equal to the depth of the soil, and the soil surface is saturated. In general, when the soil moisture increases, the pore pressure increases too and the resistant force against the landslide force decreases, so landslide is likely to commence. The classification of stability factors at different points of the domain is according to Table 1.

Table 1: Stability classification in SINMAP Model (Goodwin and Pack, 2012)

Predicted state	class	conditions
Stable slope zone	1	FS > 1.5
Moderately stable zone	2	1.5 > FS >1.25
Quasi-stable slope zone	3	1.25 > FS >1
Lower threshold slope zone	4	1 > FS > 0.5
Upper threshold slope zone	5	0.5 > FS > 0
Defended slope zone	6	FS < 0

3. Saturation Model of TOPMODEL

Topmodel is a rainfall-runoff model used to estimate surface and subsurface runoff of catchments. This model, based on the topographic index, predicts the extent of soil moisture deficit across the catchment and can identify the areas that have reached saturation. The subsurface flow saturates the soil from a lower parts of hillslope in the Dunne-Black runoff mechanism. According to this mechanism, surface runoff will flow downstream in the saturated zone, subsurface flow will flow throughout the entire hillslope, which will eventually enter the saturation zone, and all surface and subsurface runoff will enter the stream. In these circumstances, the use of Topmodel would be important to identify the points of the catchment saturated from rainfall and estimate surface and subsurface runoff.

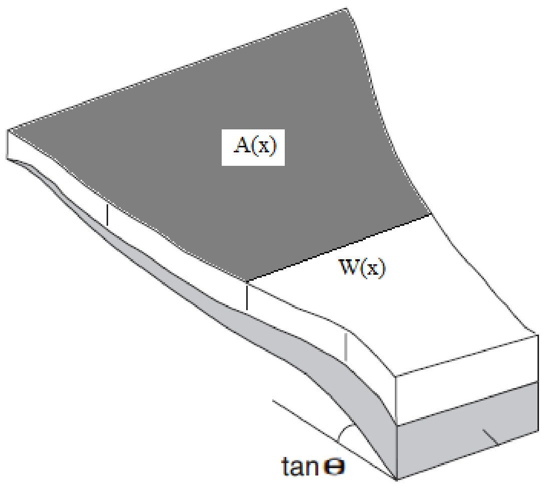

Figure 4: Hillslope’s width and upstream drainage area in each section of the hillslope

Figure (4) shows a slope affected by rainfall and its infiltration. Infiltrated water due to rainfall at section A(x) of the upstream at point x flows as a subsurface flow into the soil, and it is the subsurface flow that saturates the bottom of the slope from below. The amount of soil moisture deficit (SMD) at any point along the hillslope is computed from the following equation (1979 Beven and Kirkby):

$$D_x = \overline{D} - m\left[\lambda(x) - \overline{\lambda}\right] \qquad (4)$$

where D_x is the soil moisture deficit (SMD) to the point of saturation at point x, m is the soil reduction factor, $\overline{D}$ is the average SMD over the whole range and $\lambda(x)$ is the topographic index calculated for each point x along the hillslope by Eq. (5).

$$\lambda(x) = ln\left[\frac{a(x)}{S(x)}\right] \qquad (5)$$

where a(x) =A(x)/W(x), and S(x) = $tan(\theta_x)$ is the local slope at a distance x from the upstream. According to Fig. 3, at each section of the hillslope, A(x) is the upstream surface area above the point x, and W(x) stands for the width of the flow. Since the surface of the hillslopes is curved, the amount of slope varies locally at any point. For the sake of simplicity, we assumed the curvature of the impervious layer (i.e., the bedrock) agrees with that of the ground. a(x) is the specific area of the drainage surface above any point x on the hillslope. The upstream surface of a given point practically is the portion of the hillslope area the accumulated water from which is transferred to that point beneath the soil surface in the form of subsurface flow and may cause the saturation of that point. The parameter a(x) represents the flow accumulation at point x, and S(x) designates the flow movement.

4. Relationship between SINMAP Landslide Model and TOPMODEL

If the value of the recharge rate to the subsurface layer, R, is known, the SMD value based on Topmodel is computable from the following equation (Beven and Kirkby, 1979):

$$D_x = -m\, ln\left[\frac{Ra(x)}{T\, tan\, \theta_x}\right] \qquad (6)$$

Combining Eqs. (3) and (6), the relative saturation index δ is obtained as a function of SMD:

$$\delta x = \frac{1}{cos(\theta_x)} exp(-D_x/m) \qquad (7)$$

Eq. 7 explicitly shows the relationship between the saturation index in the SINMAP model and SMD in the Topmodel.

5. Effect of Geometry of Hillslopes on Landslide

Although, to ease the required computations, in most hydrological studies, hillslopes are considered a simple rectangular plane, defined by the slope feature, their natural geometry may vary over a wide range. In this research, two secondary aspects of hillslopes geometry are included, allowing to simulate and investigate more complex geometries: plan shape and profile curvature. In general, hillslopes are classified into three forms based on their planar forms: convergent, parallel and divergent, and based on their longitudinal curvature, into three forms:

concave, straight and convex. If these features are combined, nine complex hillslopes are achieved as shown in Figure (5).
Evans (1980) classified complex hillslopes based on their three-dimensional shapes, which consisted of the longitudinal profile or profile curvature and the plan shape of the hillslopes.
Catchment hillslopes are seen as complex ones, so it is essential to consider their three-dimensional shapes to evaluate their performance, particularly in runoff routing (response time) and stability.

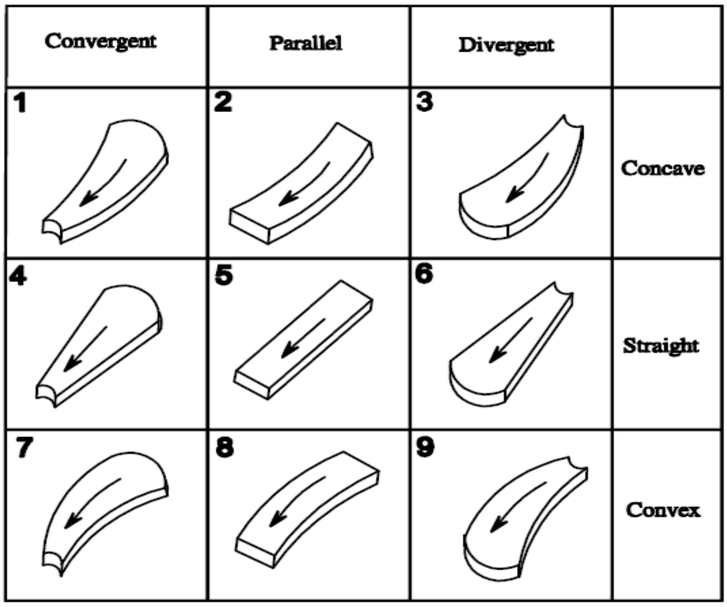

Figure 5: Three-dimensional shapes of complex hillslopes (Sabzevari et al., 2015)

According to studies done by Norbiato et al. (2008), the hillslope width function according to Fig. 3 can be considered as Eq. (8):

$$W(x) = c\, exp(\, ax) \tag{8}$$

where c is the upstream width and “a” represents the degree of convergence. For divergent, convergent, and parallel hillslopes we have, respectively, (a> 0), (a <0), and (a = 0), and the drainage surface function of the hillslopes is as Eq. (9):

$$A(x) = \frac{c}{a}[exp(\, ax) - 1] \tag{9}$$

According to Bars and Fan (1998) geometry, the equation of profile curvature in the complex hillslopes is as follows:

$$z(x) = H + \beta x + \gamma x^2 \tag{10}$$

where z(x) is the level of any point x of the hillslope relative to the datum, x measures the distance from the top of the hillslope, and the two parameters β and γ are related to the curvature of the hillslope which are determined according to the actual profile curvature. The value of γ is taken for concave hillslopes as positive, for convex hillslopes as negative, and for straight hillslopes as zero. The local slope at any point x on the hillslope is obtained from Eq. (11):

$$S(x) \quad = \left|\frac{dz}{dx}\right| = \beta + 2\gamma x \qquad (11)$$

By substituting Eqs. (8), (9), and (11) into Eq. (4), SMD at the point x of the complex hillslope can be calculated as follows:

(12)

$$D_x = \overline{D} - m\left[ln\left[\frac{a(x)}{S(x)}\right] - \overline{\lambda}\right] = \overline{D} - m\left[ln\left[\frac{(1 - exp(-ax))}{a}\right] - \overline{\lambda}\right]$$

In practice, Eq. (12) figures out the values of soil moisture deficit according to the Complex Topmodel. by substituting Eq. (12) into Eqs. (7) and (2), the magnitude of the stability factor of different points of the complex hillslopes will be calculated.

6. Dynamic TOPMODEL

Many key hydrological parameters vary spatially and temporally. Soil moisture content along the hillslopes may consistently change due to subsurface flow, and the SMD parameter varies accordingly at any point with time. Generally, first the downstream of hillslopes is saturated due to the accumulation of the subsurface flow, and subsequently, the length of the saturated zone expands towards upstream in response to the subsurface flow continuing.
The stability of the hillslopes is indeed a function of the saturation of the catchment. Thus to predict the spatial and temporal variability of the stability at different points of the hillslope, a dynamic saturation model is needed that is capable of tracing and calculating the saturation factor of each point over time.
In this regard, a Topmodel dynamic model was suggested that calculates the temporal variation of the SMD parameter and sigma parameter in the SINMAP model.

Eq. (4) is the original Topmodel equation that provides the SMD value for each surface point. In this equation, there is the parameter $\overline{D}$ which indicates the average SMD along the hillslope and whose values at each time step are calculated based on the balance equation and according to Eq. (13) (Franchini et al., 1996):

$$\overline{D}^{(t+1)} = \overline{D}^{(t)} - \left[\frac{Q_v^{(t)} - Q_B^{(t)}}{A}\right]\Delta t \qquad (13)$$

where Q_v demonstrates the recharge rate of the unsaturated zone from saturated zone over the time interval t, Q_B depicts the outflow from the subsurface store into the channel over the time interval t and $t + \Delta t$, A displays the hillslope area, and Δt is the time interval. In this regard, the values of Q_v and Q_B are calculated from Eqs. (14) and (15), respectively (Franchini et al., 1996):

(14)

$$Q_v^{(t)} = \sum_{i \in A} Q_{v_i}^{(t)} = \sum \alpha_i \, K_0 \exp\left(\frac{-\overline{D}^{(t)}}{m}\right) \qquad for\ D_i \geq 0$$

$$Q_B = A T_0 \exp(\overline{\lambda}) \exp\left(\frac{-\overline{D}^{(t)}}{m}\right) \quad (15)$$

where K_0 is the hydraulic conductivity coefficient at the ground surface, $T_0 = \frac{K_0}{f}$ shows the soil transmissivity, α_i is the area draining through location i per unit contour length (i.e., the contributing area at point *i*).

7. Results and Analysis

7.1 Effects of Geometry on Hillslopes stability

Nine complex hillslopes with different geometric features (Table 2) and hydrological characteristics of hillslopes according to Table 3 were taken into account to asses the impact of geometry on hillslopes stability,

Table 2: Geometric characteristics of hillslopes (D. Norbiato and M. Borga, 2008)

No.	Profile	Plan	β	γ	C	*a*
1	Concave	Convergent	-0.3	0.001	120	-0.038
2	Concave	Parallel	-0.3	0.001	30	0
3	Concave	Divergent	-0.3	0.001	3	0.036
4	Straight	Convergent	-0.182	0	120	-0.038
5	Straight	Parallel	-0.182	0	30	0
6	Straight	Divergent	-0.182	0	3	0.036
7	Convex	Convergent	-0.1	-0.001	120	-0.038
8	Convex	Parallel	-0.1	-0.001	30	0
9	Convex	Divergent	-0.1	-0.001	3	0.036

Table 3: Hydrologic features of hillslopes

Parameter name	Symbol	Units	Value
Effective porosity	θ_e	-	0.34
Conductivity Decay factor Hydraulic	K	m/s	0.0001
Soil reduction agent	f	-	2
m	m = θe/f	-	0.17
Soil depth(vertical)	D	m	2
Slope angle	β	deg	15
Internal friction	φ	deg	30
Saturated soil density	ρ_s	kg m^{-3}	1600
Density of water	ρ_w	kg m^{-3}	1000
Soil cohesion	c	kN m^{-2}	0

As stated before, the curvature of the impervious surface in convex and concave hillslopes affects the local slope. The local slope varies along the complex hillslopes, and as we know, the slope is an essential parameter in the stability of different parts of the hillslope. Fig. (6) illustrates the alterations of the local slope for the nine complex hillslopes using the data in Tables 2 and 3.

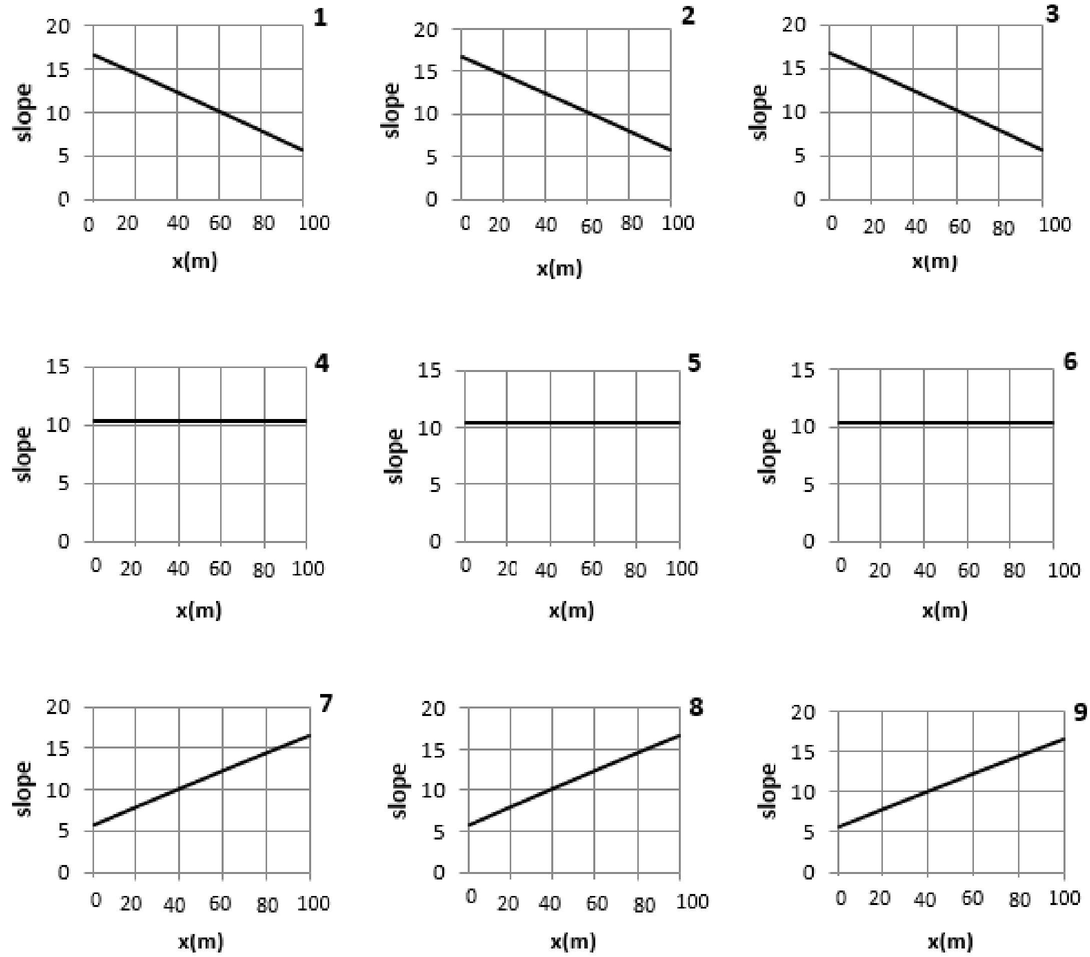

Figure 6: Variation of local slope along the hillslopes, 1-3 for convex, 4-6 for straight, and 7-9 for concave

As seen in Fig. (6), in concave hillslopes (1, 2, and 3), the slope starts from 17 and ends at 5 degrees along 100 meters. The slope for straight hillslopes (4,5,6) has a fixed value of 11 degrees. On convex hillslopes (7, 8, 9), the slope starts from 6 degrees and increases to 16, 17, and 18 degrees at distances of 98, 99 and 100 meters downstream of the convex hillslope. In general, the movement of subsurface flow is a function of the hillslope slop (e.g., in the steep slope, the concentration of subsurface flow and saturation declines), which will be examined in the sequel. As mentioned earlier, the topographic index in Topmodel is $\lambda(x) = \ln\left[\frac{a(x)}{S(x)}\right]$ equivalent to the specific catchment area index.

where a(x) represents an upstream surface of the hillslope where rainfall infiltrates and the subsurface flow from this area is concentrated in a single element of width W (x) as shown in Fig. 3. It is the ratio of the upstream area to the width of the hillslope for each point x of the hillslope. It accumulates upstream subsurface flow at any point of the hillslope (equivalent to the available water at the point), and the slope S (x) causes the upstream area to drain through the same point (equivalent to the tendency of the point to convey the available water). Therefore, the $\lambda(x)$ is a function of these two geometric features of the hillslope at any point x, significantly influencing each pixel's saturation. Each point of the slope has a saturation degree that determines the magnitude of SMD at that point. Fig. (7) shows the changes in the topographic index λ (x) for complex hillslopes in consideration of Eq. (5).

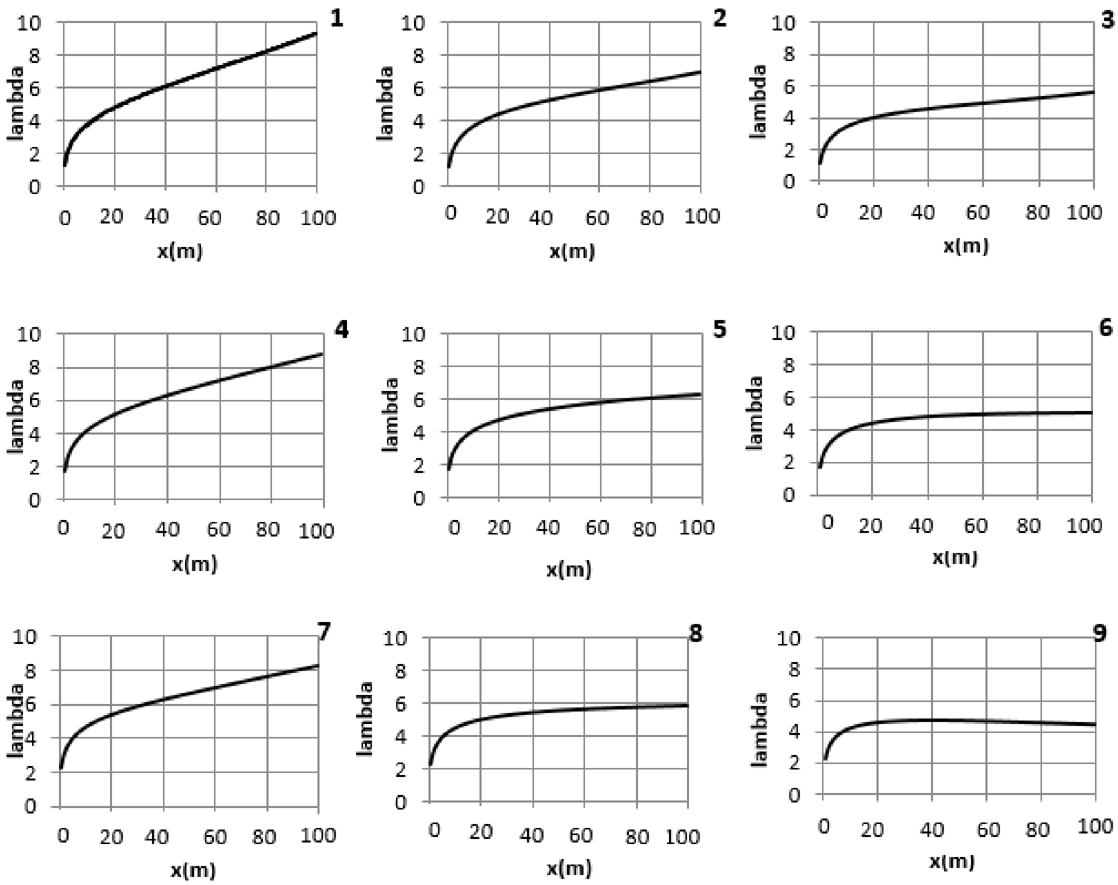

Figure 7: Topographic index of λ (x) for nine complex hillslopes

As observed in Fig. (7), the spatial distribution of λ (x) varies in different hillslopes. For example, in concave and straight hillslopes, the values of λ increase as we approach the bottom, but in convex hillslopes, the values of λ decrease at the end of the hillslope. The λ variations downstream of the concave hillslopes increase relative to the other types of hillslopes, causing subsurface flow to accumulate downstream, and saturation will naturally increase at these points. The values of λ in the convergent hillslopes are also higher than in the divergent ones. In general, changes in parameters such as slope, upstream drainage area, and λ should be considered separately at each point of the hillslope, because each point has its own characteristics.

7.2 Temporal variation and its effect on hydrological characteristics of complex hillslopes

The temporal variation and its effect on hydrological characteristics of complex hillslopes are investigated with the help of Dynamic Topmodel equations. During a rainfall event, the portion of infiltrated water runs as a lateral subsurface flow through the soil. It can saturate the downstream part of the hillslope according to the Dunne-Black mechanism. Practically, this subsurface flow increases the soil moisture in all parts of the hillslope till the saturation phase. The SMD value decreases when time increases (Fig. 8). Indeed, the saturation of the hillslopes increases over time, and as the hillslopes become more saturated, in proportion to it, a decrease in SMD values is observed. For instance, for hillslope number 3 at time $t = 0$, the SMD value is not zero at any length of the hillslope. At time $t = 2$hr about 35% of the hillslope's length (measured from downstream), and at $t = 3$hr, about 50% of the hillslope's length from downstream the SMD is equal to zero. Therefore, if rainfall continues, the whole of hillslope length moves toward saturation over time.

Here in this part of the research the effect of topography and geometry of complex hillslopes upon the subsurface hydrological response is investigated. The temporal changes of these characteristics 0, 1, 2, and 3 hours after the beginning of the rainfall using the geometry will be examined for the hillslope with the attributes listed in Tables 2 and 3 (Norbiato et al, 2008).

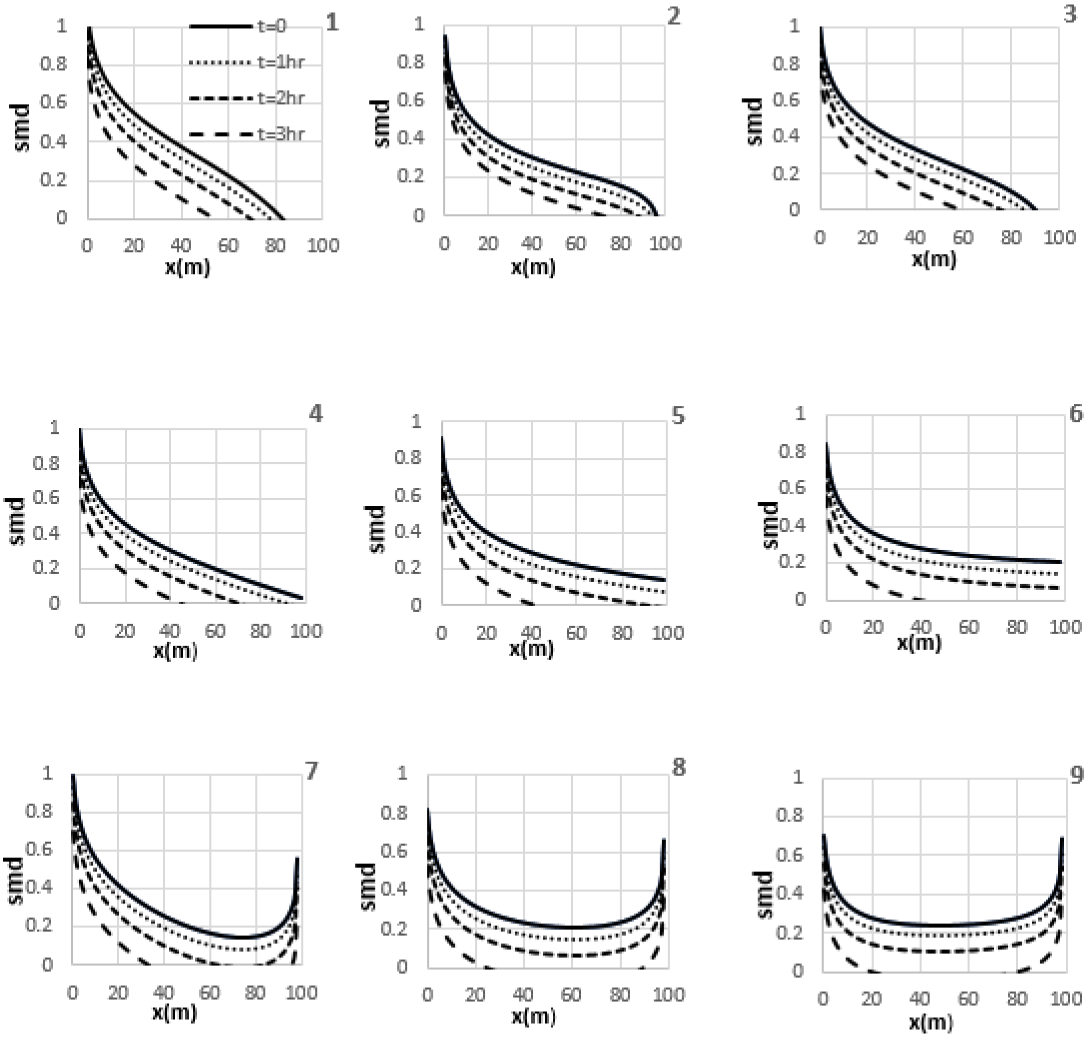

Figure 8: Spatial-temporal variation of SMD along complex hillslopes

Fig. (9) shows the temporal variation of the saturation parameter δ along the hillslopes.

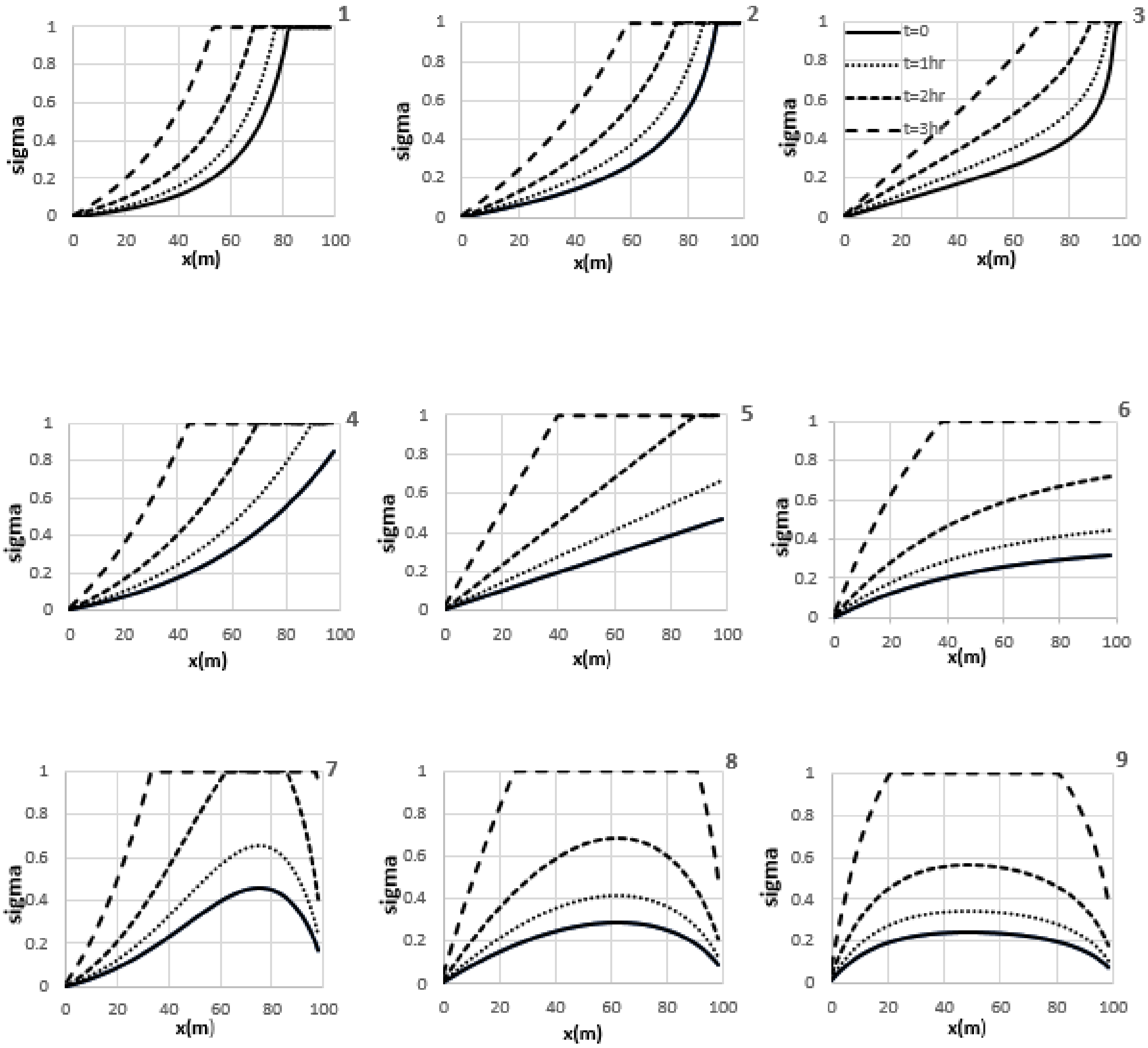

Figure 9: Spatial-temporal changes in relative saturation δ along complex hillslope versus time

The parameter δ is a function of soil saturation, which varies from 0 to 1 from upstream to downstream of the hillslopes in most hillslopes (Fig. 9). Convergent hillslopes show a higher degree of saturation than divergent and parallel ones. Therefore a bigger portion of them reaches saturation condition at downstream after 3 hours from the beginning of rainfall. In terms of profile curvature, concave hillslopes tend to be more saturated than convex and straight hillslopes (Fig. 9). The highest saturation rate was observed in convergent hillslopes (Fig. 9). In the downstream of the convex hillslopes near the outlet, the value of sigma is very low, which is associated to the topography of the hillslopes, and as can be seen, the hillslopes become more saturated over time and significantly faster in divergent ones. The stability equation of the slopes in the SINMAP model is strongly dependent on σ and the local slope angle of the hillslope, and over time the level of saturation of different points of the hillslope affects the overall stability of the hillslope. Over time, the length of the saturated zone ($\delta = 1$) will be expanded from downstream to upstream. The spatial distribution of σ over the convex hillslopes is quite different from straight or concave hillslopes (Fig. 9). It can be attributed to the exaggeratedly sharp rise in the magnitude of slope at the end of the concave surfaces defined by Bars and Fan (1998) topographic model. This feature, unique to convex surfaces, is important because it causes the downstream portion of convex hillslopes to take longer than 3 hours to become saturated.

Fig. (10) revealed the spatio-temporal variation of the stability factor (FS) along the complex hillslopes versus time.

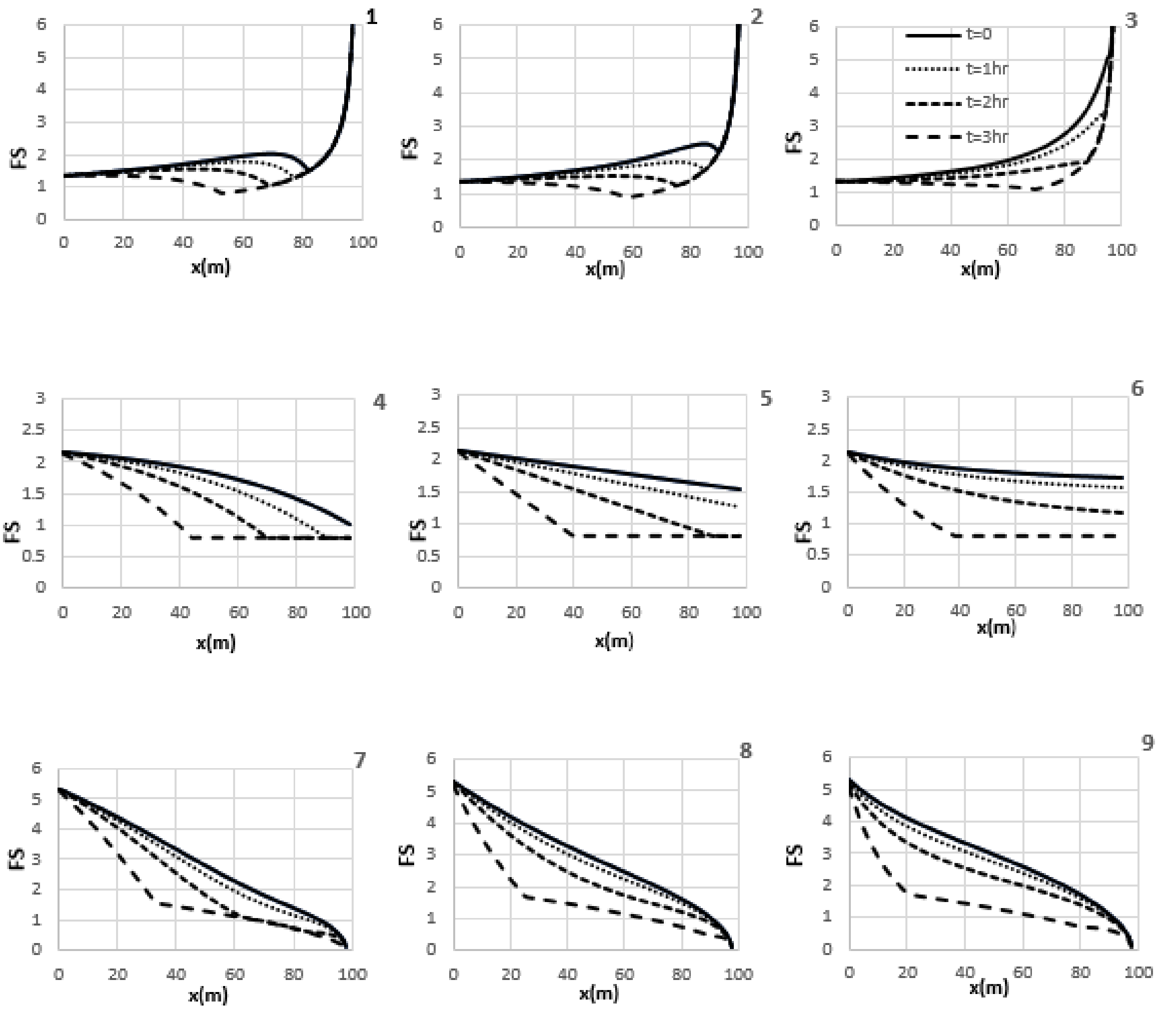

Figure (10): Spatial-temporal changes in the stability factor of complex hillslopes vs. time over the hillslope

For the concave-convergent hillslope at time t = 0, the value of FS starts from 1.5 at upstream and reaches the maximum value of 2.1 at x=75 m (Fig. 10). Afterward, over time, the downstream degree of rate increases and the SMD (Fig. 8) decreases, and the soil saturation rate (sigma) (Fig. 9), which leads to the reduction of stability versus time (Fig. 10). In this type of hillslope, the slope is decreased from upstream to downstream (Fig. 5). By saturating the downstream parts, the correspondence λ values will be increased, and instability will likely occur at the saturated zone (Fig. 9). Apparently, due to the more dominant effect of a slope than saturation, the downstream, which is mildly sloping, is shown to be stable. However, the stability disappears over time along the hillslope. While, as seen, the stability factor is linked both to the local slope angle value and the saturation index, our results indicate that the local slope plays the leading role in the stability of hillslopes.

The concave-parallel hillslopes (hillslope #2) and the concave-divergent hillslope (hillslope #3) have functioned quite similar to the concave-convergent hillslopes (hillslope #1). However, in the concave-divergent hillslope, the values of stability factor, especially in the downstream parts of the hillslope, are slightly more than the other two others. In the straight-convergent hillslope (#4), at t = 0, the FS values decrease from upstream (2.2) to downstream (1); however, Overtime (t = 1, 2, and 3 hr), the rate of instability increases (Fig. 10). At upstream, the λ values are low and vary between 1.9 and 7.5, so large amounts of λ at downstream are responsible for the instability of the hillslope #5. In the straight-parallel hillslope (#5, Fig 10), the value $1.9<FS<2.3$ changes from upstream to downstream, and the hillslope is in the stable state, while this stability will be changed over time (e.g., at t = 3 hr and x = 38 m and hillslope has turned completely unstable). In the straight-divergent hillslope (#6), at before rain rainfall (t=0), the FS changes between 2.0- 2.2, and all points of the hillslope are stable, but at t = 1, 2, 3 hr the hillslope is highly saturated and unstable (Fig. 10-6). In straight hillslopes, these are divergent hillslopes that are more stable than parallel and convergent counterparts. In the convex-convergent hillslope (#7), the FS decreases from 5.3 (upstream, stable) at onset time to 0.0 (downstream), which is in contrast to concave hillslopes (#1 to #3). It is due to the very low slope in convex hillslopes upstream and its growing towards downstream, particularly at the end of the hillslope. In addition, the values of the σ are also high at downstream of hillslope #7, with a saturation state (Fig. 8). The high slope and saturation state of the hillslope downstream has turned the stability factor to zero and leads to unstable conditions in this area. This instability expands to the middle of the hillslope after 1 hours (Fig. 10), identifying it as one of the most unstable complex hillslopes. In convex-parallel hillslope (#8), the performance is similar to hillslope #7 with more stability due to lower saturation.

8. Conclusion

The natural hillslopes of catchments have different plan shapes (convergence-divergence-parallel) and floor curvature (convex-concave-flat). In this study, the main goal was to investigate the effect of the shape and geometry of catchment hillslopes upon the saturation rate of different parts of the hillslopes and their spatial-temporal stability. The stability of the hillslopes is interrelated to the hydrological response of the subsurface flow and their saturation state. Several hillslope's geometries were transferred to Topmodel, and the Topmodel Complex model was constructed. Then, the Complex Topmodel was linked to the SINMAP landslide model for stability analysis.

The main conclusion can summeraized as:

1. The local slope varies significantly along the complex hillslopes. For example, in the concave hillslopes with different plan shapes, the local slope at upstream is high, but it decreases as it goes downstream. The convex hillslopes work oppositely. Namely, the slope is low at upstream and very high at downstream. The slope is a crucial parameter in the landslide models. As the slope increases, the concentration of subsurface flow in an element of the hillslope decreases and the saturation diminishes. Any increasing in the slope makes the reduction of the stability.

2. The topographic index in Topmodel shows the concentration of subsurface flow at any point in the hillslope and substantially affects the stability of the hillslopes. According to the results, greater values of Landa λ were observed in convergent hillslopes than in divergent ones. This parameter is affected by the shape of the plan, the local slope, and time changes.

3. The saturation index σ from Topmodel was used to evaluate the saturation extent across the hillslope. According to the results, the convergent hillslopes show more saturation than divergent and parallel hillslopes, and the concave hillslopes tend to have more saturation than the convex and straight counterparts, and saturation increases over time.

4. In the concave hillslopes with different plans (convergent, parallel, and divergent), the high and low slope in the upstream and downstream leads to lower stability factor in upstream. According to the data of this research, all points of the hillslope were in a stable state, but the downstream parts enjoyed more stability.

5. In the straight hillslope, the stability decreases from upstream to downstream. At the onset state, the lower parts of the straight-convergent hillslopes are unstable, while the whole straight-parallel and straight-divergent hillslopes are stable. Over time and increasing saturation rate, all hillslopes become more unstable.

6. The situation differs from the concave hillslopes for the convex hillslopes; the value of the stability factor at the end of the hillslope is very low. About 90% of the convex-parallel and -divergent hillslope are stable at starting state, but this percentage decreases dramatically over time and expanding saturation state across the hillslopes. Owing to the high saturation rate in the convex-convergent hillslope, the second longitudinal half of the hillslope is unstable.
7. Overall, the convex slopes divergent hillslopes are more stable than others.

Acknowledgements
This article was excerpted from a Ph.D. thesis in Water resource management, Islamic Azad University, Marvdasht Branch.

Compliance with Ethical Standards

Conflicts of interest

Authors have no conflict of interest to declare.

Ethics approval

Not applicable.

Consent to participate

Not applicable.

Consent for publication

Not applicable.

References:

Ardekani, A. A., & Sabzevari, T. (2020). Effects of hillslope geometry on soil moisture deficit and base flow using an excess saturation model. Acta Geophysica, 68(3), 773-782.

Aryal, S. K., O'Loughlin, E. M., and Mein, R. G. (2005). A similarity approach to determine response times to steady-state saturation in landscapes, Adv. Water Resour., 28, 99–115.

AVANZI G. D., GIANNECCHINI R. & PUCCINELLI A. (2004). The influence of the geological and geomorphological settings on shallow landslides. An example in a temperate climate environment: the June 19, 1996 event in northwestern Tuscany (Italy). Engineering Geology 73, 15–228.

Arnone E, Noto LV, Lepore C, Bras RL. (2011). Physically-based and distributed approach to analyze rainfall-triggered landslides at watershed scale. Geomorphology 133: 121–131.

Akbari,A., Azizan, A., and S. K. Ngien. (2016). effect of slope adjustment on curve number using global digital elevation data: new look into sharply-williams and huang methods, Second International Conference on Science, Engineering & Environment,Osaka City, Japan, Nov.21-23, 2016, ISBN: 978-4-9905958-7-6 C3051.

Berne, A., Uijlenhoet, R., & Troch, P. A. (2005). Similarity analysis of subsurface flow response of hillslopes with complex geometry. Water Resources Research, 41(9).

Bishop AW. (1959). The principle of effective stress. Tek Ukebl 106(39): 859–863.

Borga M, Dalla Fontana G, Cazorzi F. (2002). Analysis of topographic and climatologic control on rainfall-triggered shallow landsliding using a quasi-dynamic wetness index. Journal of Hydrology 268: 56–71.

Barling, R.D., Moore, I.D., Grayson, R.B. (1994). A quasi-dynamic wetness index for characterizing the spatial distribution of zones of surface saturation and soil water content. Water Resour. Res. 30 (4), 1029e1044.

Beven, K., and M. Kirkby. (1979). A physically based, variable contributing area model of basin hydrology/un mode`le a base physique de zone d'appel variable de l'hydrologie du bassin versant, Hydrol. Sci. J., 24(1), 43–69.

Cardozo, C. P., Lopes, E. S. S., & Monteiro, A. M. V. (2018). Shallow landslide susceptibility assessment using SINMAP in Nova Friburgo (Rio de Janeiro, Brazil). Revista Brasileira de Cartografia, 70(4), 1206-1230

Cho SE, Lee SR (2001) Instability of unsaturated soil slopes due to infiltration. Comput Geotech 28(3):185–208. https://doi.org/10. 1016/S0266-352X(00)00027-6

Cascini L, Cuomo S, Pastor M, Sorbino G. (2010). Modeling of rainfall induced shallow landslides of the flow-type. J Geotech Geoenviron 136(1):85–98. https://doi.org/10.1061/(ASCE)GT.1943-5606. 0000182.

Campos TMP, Andrade MHN, Gerscovich DMS, Vargas Jr. EA. (1994). Analysis of the failure of an unsaturated gneissic residual soil slope in Rio de Janeiro, Brazil. 1st Panamerican Symposium On Landslides, pp. 201–213.

Cerdà, A., García-Fayos, P. (1997). The influence of slope angle on sediment, water and seedlosses on badland landscapes. Geomorphology 18(2), 77-90.

Chen, L., Young, M.H. (2006). Green-Ampt Infiltration Model for Sloping Surfaces. WaterResour. Res. 42, W07420.

Chaplot, V., Le Bissonais, Y. (2000). Field measurements of interrill erosion under different slopes and plot sizes. Earth Surf. Process. Landforms 25, 145-153.

Dai FC, Lee CF, Ngai YY. (2002). Landslide risk assessment and management: an overview. Eng Geol 64(1):65–87. https://doi.org/10.1016/S0013-7952(01)00093-X

Dilley, M., Chen, R.S., Deichmann, U., Lerner-Lam, A., Arnold, M., Agwe, J., Buys, P., Kjekstad, O., Lyon, B., Yetman, G. (2005). Natural disaster hotspots: A global risk analysis. World Bank Disaster Risk Management Series.

Dunne, T., and R. D. Black. (1970). An experimental investigation of runoff production in permeable soils, Water Resour. Res., 6, 478 – 490.

Djorovic, M. (1980). Slope effect on runoff and erosion, in Assessment of Erosion, edited by M. De Boodt and D. Gabriels, pp. 215– 225, JohnWiley, Hoboken, N. J.

De Ploey, J., J. Savat, and J. Moeyersons. (1976). The differential impact of some soil loss factors on flow, runoff creep and rainwash, Earth Surf. Processes Landforms, 1, 151– 161.

Evans IS. (1980). An integrated system of terrain analysis and slope mapping. Zeitschrift fur Geomorphologie, Supplementband 36: 274-295.

Fariborzi, H., Sabzevari, T., Noroozpour, S., & Mohammadpour, R. (2019). Prediction of the subsurface flow of hillslopes using a subsurface time-area model. Hydrogeology Journal, 27(4), 1401-1417.

Fernandes NF, Guimarães RF, Gomes RAT, et al. (2004). Topographic controls of landslides in Rio de Janeiro: field evidence and modeling. Catena 55: 163-181.

Fox, D.M., Bryan, R.B., Price, A.G. (1997). The influence of slope angle on final infiltrationrate for interrill conditions. Geoderma 80, 181-194.

Gao J, Maro J. (2010). Topographic controls on evolution of shallow landslides in pastoral Wairarapa, New Zealand, 1979- 2003. Geomorphology 114: 373-381.

Govers, G. (1991). A field study on topographical and topsoil effects on runoff generation, Catena, 18, 91– 111.

Grosh, J. L., and A. R. Jarrett. (1994). Interrill erosion and runoff on verysteep slopes, Trans. ASAE, 37(4), 1127– 1133.

Godt JW, Baum RL, Lu N. (2009). Using soil suction and moisture content measurements for landslide prediction. Geophysical Research Letters 36: L02403. DOI: 10.1029/2008GL035996.

Hilberts, A., Van Loon, E., Troch, P. A., and Paniconi, C. (2004). The hillslope-storage Boussinesq model for non-constant bedrockslope, J. Hydrol., 291, 160–173.

Hammond, C., Hall, D., Miller, S., Swetik, P. (1992). Level I Stability Analysis (LISA) documentation for version 2.0. USDA Forest Service Intermountain Research Station, General Technical Report INT-285.

Ha, N. D., Sayama, T., Sassa, K., Takara, K., Uzuoka, R., Dang, K., & Van Pham, T. (2020). A coupled hydrological-geotechnical framework for forecasting shallow landslide hazard—a case study in Halong City, Vietnam. Landslides, 1-16.

Hilberts A, Troch PA, Paniconi C, Boll J. (2007). Low-dimensional modeling of hillslope subsurface flow: the relationship between rainfall, recharge, and unsaturated storage. Water Resour Res 43:W03445. doi:10.1029/2006WR006496.

IIDA T. (1999). A stochastic hydro-geomorphological model for shallow landsliding due to rainstorm. Catena 34, 293–313.

Janeau, J.L., Bricquet, J.P., Planchon, O., Valentin, C. (2003). Soil crusting and infiltration on steep slopes in northern Thailand. Europ. J. Soil Sci. 54,543-553.

Kjekstad, O., & Highland, L. (2009). Economic and social impacts of landslides. In Landslides–disaster risk reduction. Springer, Berlin, Heidelberg (pp. 573-587).

Kim MS, Onda Y, Uchida T, Kim JK, Song YS. (2018). Effect of seepage on shallow landslides in consideration of changes in topography: case study including an experimental sandy slope with artificial rainfall. CATENA 161:50–62. https://doi.org/10.1016/j.catena. 2017.10.004.

Kim, M. S., Onda, Y., Kim, J. K., & Kim, S. W. (2015). Effect of topography and soil parameterisation representing soil thicknesses on shallow landslide modelling. Quaternary International, 384, 91-106.

Kirkby, M.J. (1997). TOPMODEL: a personal view. Hydrol. process. 11 (9), 1087e1097.

Lamb, R., Beven, K. (1997). Using interactive recession curve analysis to specify a general catchment storage model. Hydrol. Earth Syst. Sci. Discuss. 1 (1), 101e113.

Lin, Q., Wang, Y. (2018). Spatial and temporal analysis of a fatal landslide inventory in China from 1950 to 2016. Landslides 15, 2357–2372.

Lu N, Godt J. (2013). Hill slope hydrology and stability. Cambridge University Press, New York.

Liang, W. L., & Chan, M. C. (2017). Spatial and temporal variations in the effects of soil depth and topographic wetness index of bedrock topography on subsurface saturation generation in a steep natural forested headwater catchment. Journal of Hydrology, 546, 405-418.

Lane, S.N., Brookes, C.J., Kirkby, M.J., Holden, J. (2004). A network-index-based version of TOPMODEL for use with high-resolution digital topographic data. Hydrol. Process. 18 (1), 191e201.

Lal, R. (1976). Soil erosion of Alfisols in western Nigeria: Effects ofslope, crop rotation and residue management, Geoderma, 16, 363–375.

Michel, G. P., Kobiyama, M., & Goerl, R. F. (2014). Comparative analysis of SHALSTAB and SINMAP for landslide susceptibility mapping in the Cunha River basin, southern Brazil. Journal of soils and sediments, 14(7), 1266-1277.

Montgomery, D.R., Dietrich, W.E. (1994). A physically based model for the topographic control on shallow landsliding. Water Resources Research 30, 1153–1171.

Morbidelli, R., Saltalippi, C., Flammini, A., Cifrodelli, M., Corradini, C., Govindaraju, R.S. (2015). Infiltration on sloping surfaces: Laboratory experimental evidence and implicationsfor infiltration modelling. J. Hydrol. 523, 79-85.

Morbidelli, R., Saltalippi, C., Flammini, A., Cifrodelli, M., Picciafuoco, T., Corradini, C.,Govindaraju, R.S. (2016). Laboratory investigation on the role of slope on infiltration overgrassy soils. J. Hydrol. 543, 542-547.

Mah, M. G. C., L. A. Douglas, and A. J. Ringrose-voase. (1992). Effects ofcrust development and surface slope on erosion by rainfall, Soil Sci., 154,37– 43.

Moore, I.D., Grayson, R.B., Ladson, A.R. (1991). Digital terrainmodelling: a review of hydrological, geomorphological, andbiological applications. Hydrolog. Processes 5, 3±30.

Mishra & Anubhav Chaudhary & Raj Kaji Shrestha &Ashish Pandey & Mohan Lal. (2014). Experimental Verification of the Effect of Slope and Land Use on SCS Runoff Curve Number, Water Resour Manage 28:3407–3416 DOI 10.1007/s11269-014-0582-6.

Ng, C. W. W., & Shi, Q. (1998). A numerical investigation of the stability of unsaturated soil slopes subjected to transient seepage. Computers and geotechnics, 22(1), 1-28.

Nassif, S.H., Wilson, E.M. (1975). The influence of slope and rain intensity on runoff and infiltration. Hydrol. Sci. Bull. 20(4), 539-553.

Nachabe, M.H. (2006).Equivalence between TOPMODEL and the NRCS curve number method in peredicting variable runoff source areas. Journal of the american water resources association.

O'loughlin, E. M. (1986). Prediction of surface saturation zones in natural catchments by topographic analysis. Water Resources Research, 22(5), 794-804.

Ogden, F. L., & Watts, B. A. (2000). Saturated area formation on nonconvergent hillslope topography with shallow soils: A numerical investigation. Water Resources Research, 36(7), 1795-1804.

Pack, R. T., Tarboton, D. G., & Goodwin, C. N. (2001). Assessing terrain stability in a GIS using SINMAP.

Pack, R. T., Tarboton, D. G., & Goodwin, C. N. (1998). Terrain stability mapping with SINMAP, technical description and users guide for version 1.00.

Pack, R. T., Tarboton, D. G., & Goodwin, C. N. (1998). The SINMAP approach to terrain stability mapping.

Park HJ, Lee JH, Woo I. (2013). Assessment of rainfall-induced shallow landslide susceptibility using a GIS-based probabilistic approach. Eng Geol 161:1–15. https://doi.org/10.1016/j.enggeo.2013.04.011.

Pack RT, Tarboton DG, Goodwin CN. (1998). Terrain stability mapping with SINMAP, technical description and users guide for version 1.00. Report Number 4114–0, Terratech Consulting Ltd., Salmon Arm, Canada, 68 p.

PACK, R. T.; TARBOTON, D. G.; GOODWIN, C. N. (1999). GIS-based landslide susceptibility mapping with SINMAP. Proceedings of the 34th Symposium on Engineering Geology and Geotechnical Engineering. BAY, J. A. (Ed.). Logan, pp. 219-231.

Park, S. J., McSweeney, K., and Lowery, B. (2001). Identification of the spatial distribution of soils using a process-based terrain characterization. Geoderma, Vol. 103, pp. 249-272.

Poesen, J. (1984). The influence of slope angle on infiltration rate and Hortonian overland flow. Zeitschrift für Geomorpholgie, Supplement Band, 49, 117-131.Philip, J.R., 1991. Hillslope Infiltration: Planar Slopes. Water Resour. Res. 27(1), 109-117.

Philip JR. (1991a). Hillslope infiltration: divergent and convergent slopes. Water Resour Res 27:1035–1040.

Philip JR. (1991b). Infiltration and downslope unsaturated flows in concave and convex topographies.Water Resour Res 27:1041–1048.

Pishvaei, M. H., Sabzevari, T., Noroozpour, S., & Mohammadpour, R. (2020). Effects of hillslope geometry on spatial infiltration using the TOPMODEL and SCS-CN models. Hydrological Sciences Journal, 65(2), 212-226.

PRETI, F.; LETTERIO, T. (2015). Shallow landslide susceptibility assessment in a datapoor region of Guatemala (Comitancillo Municipality). Journal of Agricultural Engineering, vol. 46, n. 3, pp. 85-95.

RABONZA, M. L.; FELIX, R. P.; LAGMAY, F.; ECO, R. N. C.; ORTIZ, I. J. G.; AQUINO, D. T. (2016). Shallow landslide susceptibility mapping using high resolution topography for areas devastated by supertyphoon Haiyan. Landslides, vol. 13, pp. 201-210.

Rogers, C. T. and Sitar, N. (1993). Expert systems approach to regional evaluation of debris flow hazard, Geotechnical Engineering Report No. UCB/GT/93-08, Geotechnical Engineering Department of Civil Engineering, University of California, Berkeley.

Ribolzi, O., Hermida, M., Karambiri, H., Delhoume, J.P., Thiombiano, L. (2006). Effects of aeolian processes on water infiltration in sandy Sahelian rangeland in Burkina Faso.Catena 67, 145–154.

Ribolzi, O., Patin, J., Bresson, L., Latsachack, K., Mouche, E., Sengtaheuanghoung, O.,Silvera, N., Thiébaux, J.P., Valentin, C. (2011). Impacy of slope gradient on soil surfacefeatures and infiltration on steep slopes in northern Laos. Geomorphology 127(1-2), 53-63.

Sabzevari, T., Talebi, A., Ardakanian, R., & Shamsai, A. (2010). A steady-state saturation model to determine the subsurface travel time (STT) in complex hillslopes. Hydrology and Earth System Sciences, 14(6), 891-900.

Sabzevari, T., & Noroozpour, S. (2014). Effects of hillslope geometry on surface and subsurface flows. Hydrogeology journal, 22(7), 1593-1604.

Sabzevari, T., & Talebi, A. (2021). Landslide hazard zonation of catchments by using TOPMODEL and SINMAP models. Watershed Engineering and Management, 13(1), 222-234.

Safaei M, Omar H, Huat BK, Yousof ZBM, Ghiasi V. (2011). Deterministic rainfall induced landslide approaches, advantage and limitation. Electron J Geotech Eng 16:1619–1650.

Sharma, R. H. (2013). Evaluating the effect of slope curvature on slope stability by a numerical analysis. Australian Journal of Earth Sciences, 60(2), 283-290.

Sharma, K., O. Pareek, and H. Singh. (1986). Microcatchment water harvestingfor raising Jujube orchards in an arid climate, Trans. ASEA, 29(1), 112– 118.

Sharma, K., Singh, H., Pareek, O. (1983). Rain water infiltration into a bar loamy sand. Hydrol. Sci. J. 28, 417-424.

Shrestha, R.K., Mishra, S.K., and Pandey, A. (2013). Curvenumberaffected by slope of experimental plot having maize crop.Journal of IndianWater Resources Society, 33 (2), 42–50.

Sabzevari, T., Noroozpour, S., Pishvaei, M. (2015). Efects of geometry on runoff time characteristics and time-area histogram of hillslopes, Elsevier, Journal of hydrology,531, 638-648.

Sabzevari T, Talebi A, Ardakanian R, Shamsai A. (2010). A steady state saturation model to determine the subsurface travel time (STT) in complex hillslopes. Hydrol Earth Syst Sci 14:891–900. doi:10.5194/hess-14-891-2010.

Sabzevari, T., Noroozpour, S., & Pishvaei, M. H. (2015). Effects of geometry on runoff time characteristics and time-area histogram of hillslopes. Journal of Hydrology, 531, 638-648.

Troch, P. A., Paniconi, C., & Emiel van Loon, A. E. (2003). Hillslope-storage Boussinesq model for subsurface flow and variable source areas along complex hillslopes: 1. Formulation and characteristic response. Water Resources Research, 39(11).

Talebi, A., Uijlenhoet, R., & Troch, P. A. (2008). A low-dimensional physically based model of hydrologic control of shallow landsliding on complex hillslopes. Earth Surface Processes and Landforms: The Journal of the British Geomorphological Research Group, 33(13), 1964-1976.

Talebi A, Uijlenhoet R, Troch PA. (2008). A low-dimensional physically based model of hydrologic control of shallow landsliding on complex hillslopes. Earth Surface Processes and Landforms 33: 1964-1976.

TAROLLI, P.; TARBOTON, D. G. (2006). A new method for determination of most likely landslide initiation points and the evaluation of digital terrain model scale in terrain stability mapping. Hydrology and Earth System Science, vol. 10, 663-677.

TARBOTON, D. G. (1997). A new method for the determination of flow directions and contributing areas in grid digital elevation models. Water Resources Research, vol. 33, n. 2, 309-319.

Talebi, A., Troch, P.A., Uijlenhoet, R. (2008). A steady-state analytical hillslope stability model fo complex hillslopes. Hydrol. Process., 22, 546–553.

Troch PA, van Loon AH, Hilberts AGJ. (2002). Analytical solutions to a hillslope storage kinematic wave equation for subsurface flow. Adv Water Resour 25(6):637–649.

Troch PA, Paniconi C, Van Loon E. (2003). Hillslope-storage Boussinesq model for subsurface flow and variable source areas along complexhillslopes: 1. formulation and characteristic response. Water ResourRes 39(11):1316. doi:10.1029/2002WR001728.

Ward, R.C., 1967. Principles of Hydrology. McGraw-Hill, London, 403 pp.Watson, K.K. (1965). A statistical treatment of the factors affecting the infiltration capacity of field soils. J. Hydrol., 3: 38-65.

Wang, J., Chen, L., Yu, Z. (2018). Modeling rainfall infiltration on hillslopes using fluxconcentration relation and time compression approximation. J. Hydrol. 557, 243-253.

Wu W, Sidle R. (1995). A distributed slope stability model for steep forested basins. Water Resources Research 31: 2097–2110.

Zhang LL, Zhang J, Zhang LM, Tang WH. (2011). Stability analysis of rainfall induced slope failure: a review. Proc ICE-Geotech Eng 164(5):299–316.

ZIZIOLI, D.; MEISINA, C.; VALENTINO, R.; MONTRASIO, L. (2013). Comparison between different approaches to modeling shallow landslide susceptibility: a case history in Oltrepo Pavese, Northern Italy. Natural Hazards and Earth System Science, vol. 13, 559-573.